Fatigue Behavior of Acrylic Interpenetrating Polymer Networks. II

T. HUR, J. A. MANSON,* R. W. HERTZBERG,†
and L. H. SPERLING, *Center for Polymer Science and Engineering, Department of Chemical Engineering, Materials Research Center, Whitaker Laboratory #5, Lehigh University, Bethlehem, Pennsylvania 18015*

Synopsis

Energy-absorbing simultaneous interpenetrating networks (SINs) based in polyether-type polyurethanes (PUs) and poly(methyl methacrylate) (PMMA) networks were prepared by a prepolymer procedure. The products are translucent and appear to have single and broad glass transitions, suggesting some degree of phase separation. The percent energy absorption determined from dynamic properties and pendulum impact tests, the resistance to fatigue crack growth and fracture toughness (K_{1c}) all increase with polyurethane content. The fracture behavior changes from brittle to ductile failure with increasing PU. The fatigue fracture surfaces of the SINs show extensive stress whitening associated with cavitation around the polyurethane domains, and localized shear deformation rather than crazing.

INTRODUCTION

The ever-increasing demand for new engineering plastics has led to a flourishing interest in interpenetrating polymer networks (IPNs) of various kinds from both the scientific and technological viewpoints.[1-3] IPNs are combinations of crosslinked polymers containing fewer grafts between the networks than crosslinks within the networks. By combining elastomeric and plastic components in the form of IPNs, interesting synergisms such as improved tensile and tear strengths[4-7] and damping characteristics[8-13] have been obtained. These properties depend significantly on the morphology, which in turn is affected by the method of synthesis.[2,12]

Most combinations of polymer pairs are immiscible due to their very small entropy and positive heat of mixing. Mechanical blending of polymers often results in a coarse multiphase morphology. However, in the case of IPNs, if mixing is accomplished simultaneously with crosslinking, phase separation may be kinetically controlled by permanent interlocking of entangled chains.[3,6] Thus, the resulting domain sizes range from a few micrometers to a few tens of nanometers and finally to those with no resolvable domain structure, depending on the competition of the thermodynamic considerations and whether or not gelation preceeds phase separation.

By way of review, elastomeric phases include a variety of polymers such as rubbery acrylics, polyesters, and polyurethanes. Among these, polyurethanes

*Posthumously.
†Department of Materials Science and Engineering.

Journal of Applied Polymer Science, Vol. 39, 1933–1947 (1990)
 CCC 0021-8995/90/091933-15$04.00

have been investigated as energy-absorbing materials in orthopedic applications, such as athletic footwear, and sound and vibration damping.[14] In such polyurethanes it is desirable to modify properties over a wide range of hardness and resilience; the polyurethanes themselves are of inherent interest as toughening phases for brittle matrices. Therefore, in the form of full IPNs, polyurethanes have received much attention as the rubbery phase,[4-8,10-13,15-18] combined with crosslinked polymers such as polystyrene,[15] unsaturated polyester,[16] epoxies,[8,11] poly(vinyl acetate),[17] polyacrylate,[6,7,10] and PMMA.[4,5,13,18] Semi-IPNs have also been based on polyurethanes with poly(methyl acrylate),[19] poly(vinyl acetate),[17] and PMMA.[4,5] Both two phase[4,18] and single-phase systems[5,11] have also been reported, and at least in some cases, synergistic improvements in tensile, lap-shear and tear strengths have been found.[4,6]

PU and PMMA have been combined very often as IPNs, mainly because these polymers are already widely used in the plastics industry. Frisch and co-workers[18] investigated PU/PMMA SINs and showed that the interesting mechanical behavior of these combinations was due to a greater interpenetration of the two component phases as compared to the corresponding mechanical blends or the so-called semi-IPNs. Allen et al.[20,21] showed that these materials improved impact and shear resistance. Also, it was demonstrated that the domain size derived from the turbidity equation agreed with those observed by low angle X-ray scattering (LAXS) and electron microscopy.[22] Meyer et al. studied the mechanical properties,[4] and the chemical aspects of synthesis,[23] namely the occurrence of unwanted side reactions, and the kinetics of network formation.

Lipatov et al.[24] examined the interfacial behavior of PU/PMMA IPNs. The excess free volume in the transition layer can lead to an IPN with reduced density.

Recently, Mai and Johari[25] examined the effect of physical aging of these materials. The densification due to aging of the PMMA network influenced the relaxation kinetics of PU network. Thus, the α peak of PU was shifted towards higher temperatures.

Because of the current trend toward the use of IPNs in engineering applications, consideration of the possible consequences of exposure to fatigue loading is extremely important.[26] Such information is useful from an engineering viewpoint in that it allows the designer the opportunity to predict fatigue life and overall cyclic response of numerous polymeric solids. Fatigue measurements may be conducted using either notched or unnotched specimens. While the use of unnotched specimens does not usually distinguish between the initiation and propagation stages, the use of notched specimens concentrates solely on the crack propagation stage. Fatigue crack propagation (FCP) studies with notched specimens constitute a conservative approach to the problems of failure, since the use of a notch to simulate the presence of a defect implies that real materials do contain defects that may grow into catastrophic cracks.

Qureshi et al.[27] have reported that simultaneous interpenetrating networks, SINs, based on combinations of rubbery polyesters (derived from botanical oils) with crosslinked polystyrene (PS) were significantly superior in FCP

resistance to the PS control. In this respect, the SINs were a new type of rubber-toughened plastics.

Previous studies in this laboratory described the energy absorption and fatigue behavior of SINs based on polyurethane (PU) and poly(methyl methacrylate) (PMMA) made by a one-shot procedure, paper I in this series.[28] The one-shot procedure was accomplished by quiescent polymerization of the PU reactants with MMA plus a crosslinking agent. The energy absorption values increased directly with the PU content. Good correlations between quite variable states of stress and both linear and nonlinear viscoelastic behavior were obtainable over the whole range composition. Fatigue crack propagation (FCP) resistance was improved with PU content up to 50%, the limit characterizable with current equipment. At higher polyurethane concentrations, it was not possible to obtain stable crack growth without instrumentation specifically designed for elastomers. Although the values of energy absorption do not correspond to values of the strain energy release rate, the fatigue parameters ΔK^* (the values of stress intensity factor range, ΔK, corresponding to an arbitrary crack speed) and the crack growth rate, da/dN, at constant ΔK correlated well with energy absorption.

In view of these promising results, similar SINs were prepared, but in which the PU was prepolymerized prior to mixing with a PMMA prepolymer. This paper describes the synthesis and characterization of a series of *cross*-polyurethane-*inter-cross*-poly(methyl methacrylate), PU/PMMA, SINs made by the prepolymer procedure and an evaluation of their fatigue crack propagation behavior.

EXPERIMENTAL

Synthesis

Diphenyl methane 4,4′-diisocyanate (MDI), poly(oxypropylene glycol) (PPG) of molecular weight 2000, and trimethylol propane (TMP) were vacuum dried at 80°C for 5 h. Methyl methacrylate (MMA) (laboratory reagent) was freed from inhibitor and water by passing through a neutral alumina column and molecular sieves. The crosslinking points of each network were introduced via trifunctional polyols (for the PU network) and tetramethylene glycol dimethacrylate (TEGDM) (for the PMMA network).

The isocyanate-terminated PU prepolymer was prepared by reacting two equivalent weights of MDI with one equivalent weight of PPG at room temperature for 1 h. Since the PPG may react with both groups on the MDI, some chain extension is expected, with oligomers of the prepolymer coexisting with the di-MDI-mono-PPG product, and some free MDI. Indeed, a viscosity increase was noted. The PU prepolymer was stored under vacuum (for not more than 1 day) because of its susceptibility to moisture.

The mixture of MMA, TEGDM, and initiator was reacted until 10–15% conversion of the MMA, at which point the reaction was stopped by rapid cooling. Then the PU prepolymer, MMA prepolymer, and TMP were homogeneously mixed using a high-torque stirrer. The air entrapped during mixing

was removed by applying a vacuum for 30 s, and the mixture was poured into a mold. After gelation, the casting was cured at 60°C for 48 h.

Instrumentation and Experimental Procedure

Dynamic mechanical spectra were obtained at 110 Hz using an Autovibron unit, Model DDV-IIIC over a temperature range from −100 to 200°C at a programmed heating rate of 1°C/min; values of T_g were obtained from the temperatures corresponding to the maxima in the loss modulus (E'') peaks. The shear modulus G was also measured at room temperature using a Gehman torsional tester.

The percent energy absorbed, $E(\text{abs})$,

$$E(\text{abs}) = \frac{100E(\text{abs})}{[E(\text{abs}) + E(\text{recovered})]} \tag{1}$$

was determined in several ways: (1) using a Zwick pendulum tester to obtain the percent rebound resilience R (% energy absorbed = 100 − R); (2) using a computerized Instron tester (Model 1332) to obtain hysteresis loops under cyclic compression at 10 Hz; and (3) using dynamic mechanical data to calculate the ratio of energy absorbed to energy input (per quarter cycle), given by $1/[1 + (2/\pi \tan \delta)]$.[29]

Fatigue tests were conducted on standard-geometry compact tension specimens (6.35 cm × 6.1 cm × 6 mm) using a closed-loop electrohydraulic testing machine under ambient conditions. Specimens were precracked at 100 Hz until a stable crack front was established, and the actual crack growth data were recorded at a sinusoidal frequency of 10 Hz. All testing was performed with an R value of 0.1 (R = min/max load). The crack length, a, was measured using a traveling microscope, or, in some cases, by computer (using a compliance technique).

The range of stress-intensity factor ΔK, a measure of the driving force for crack extension, was calculated using the formula

$$\Delta K = Y\Delta\sigma\sqrt{a} \tag{2}$$

where $\Delta\sigma$ = stress range = $\Delta P/tw$, ΔP = load range, t = specimen thickness, w = specimen width, a = crack length, and Y = geometric correction factor, $f(a/w)$. The crack growth rate at a particular point was calculated to be the average crack growth rate from the previous to the succeeding point; that is,

$$\left(\frac{da}{dN}\right)_n = \frac{a_{n+1} - a_{n-1}}{N_{n+1} - N_{n-1}} \tag{3}$$

where N is the total number of cycles at the time of each crack-tip reading. Values of log da/dN were plotted against log ΔK. This plot reflects the Paris equation[30]:

$$da/dN = A\,\Delta K^m \tag{4}$$

where A and m are constants.

The fracture surfaces of the SINs were examined in the ETEC autoscan scanning electron microscope at a relatively low beam current and accelerating voltage of approximately 20 kV. Prior to examination, the surfaces were coated with a thin evaporated layer of gold in order to improve conductivity and prevent charging.

The fracture toughness, K_{1c}, was determined from three-point bend specimen[31] using ASTM Standards E 399 at a strain rate of 10 mm/s; values reported are the average for three specimens.

RESULTS

Characterization of Polymers

The SIN samples appeared translucent to the eye; hence some degree of phase separation is indicated. The dynamic mechanical data show a single broad transition which depends on composition (Fig. 1). The transitions for all the SINs are broader than for the two homopolymers. The corresponding tan δ values are shown in Figure 2. The shoulder of tan δ in the midrange compositions suggests a considerable extent of phase separation.

As expected, the T_g, based on E'' peaks varies with composition (Table I). However, Figure 3 shows that values are always lower than those predicted by the Fox[32] and Pochan equations,[33] i.e.,

Fox equation:

$$1/T_g = w(\mathrm{A})/T_g(\mathrm{A}) + w(\mathrm{B})/T_g(\mathrm{B}) \tag{5}$$

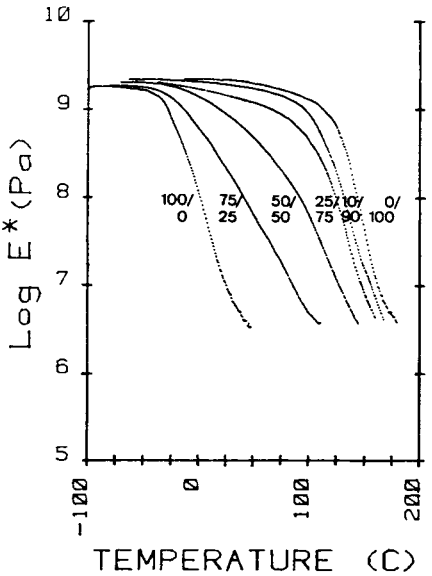

Fig. 1. Complex modulus for prepolymer PU/PMMA SINs as a function of temperature.

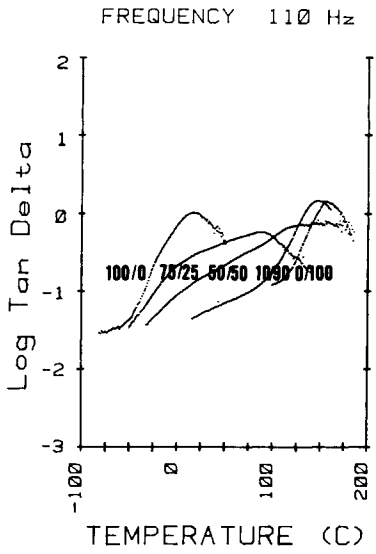

Fig. 2. Tan δ for prepolymer PU/PMMA SINs as a function of temperature.

Pochan equation:

$$\ln T_g = w(\mathrm{A}) \ln T_g(\mathrm{A}) + w(\mathrm{B}) \ln T_g(\mathrm{B}) \tag{6}$$

where w is the weight fraction and A and B refer to the two homopolymers involved.

The shear modulus at 25°C also varies with composition and is compared with the predictions of several models (see Fig. 4). These include models of Takayanagi[34] (series-parallel type), Davies[35] (especially suited to dual-phase continuity), Budiansky[36] (phase inversion at the mid-range compositions), and Hourston and Zia[19] (a modified Davies equation). As shown in Figure 4, the values fall between the Davies and Budiansky models. This suggests that dual phase continuity exists in the midrange compositions.

Energy absorption, E(abs), data are presented in Table I. Clearly the energy absorption values for the SINs increase directly with the PU content.

TABLE I
Properties of PU/PMMA SINs made by Prepolymer Procedure

PU/PMMA	T_g (°C) (110 Hz)	tan δ (25°C)	E(abs) (%) DMS	Hysteresis	Pendulum	K_{1c}^a (MPa$\sqrt{\text{m}}$)
0/100	121	0.07	9.9	54	12.0	1.43
10/90	100	0.08	11.2	58	13.3	1.53
25/75	63	0.1	13.5	64	16.1	1.65
50/50	16	0.148	18.9	70	27.3	1.73
75/25	−9	0.324	33.7	80	56.7	—
100/0	−24	0.93	59.4	85	59.0	—

[a]ASTM E399; strain rate 10 mm/s.

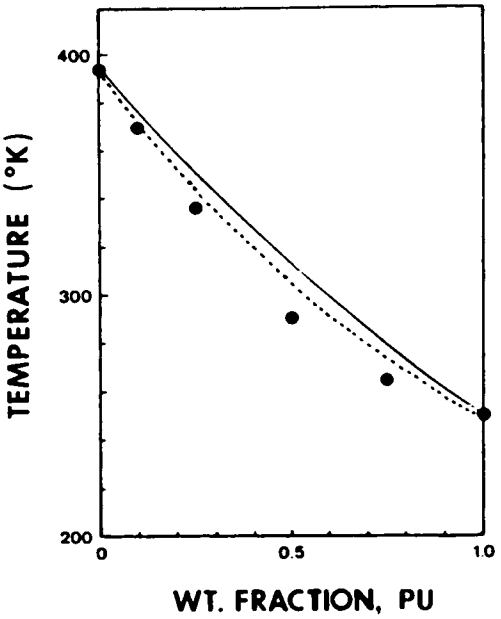

Fig. 3. Glass transition temperature as a function of composition for PU/PMMA SINs: (- - -) Fox equation (26): (—) Pochan equation (27).

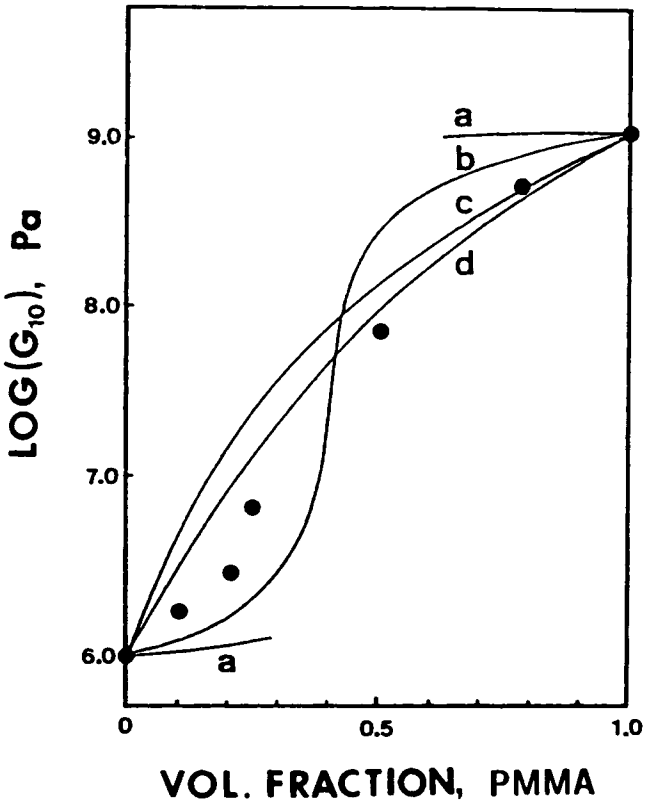

Fig. 4. Shear modulus as a function of composition for PU/PMMA SINs. Models of: (a) Takayanagi[34]; (b) Budiansky[36]; (c) Davies[35]; (d) Hourston and Zia.[19]

Fatigue Crack Propagation

Fatigue crack propagation (FCP) resistance significantly improved with increasing PU content (Fig. 5). Unfortunately, when the amount of PU was larger than 50%, the FCP resistance could not be measured, since the material's stiffness was too low.[26,37]

As shown in Figure 6, the driving force for crack extension ΔK^* (the value of ΔK corresponding to an arbitrary crack speed, in this case 10^{-3} mm/cycle) was increased from 0.7 to 1.2 as the PU content was increased from zero to 50%. This means a factor of 2 increase in required driving force.

Fracture Toughness

The fracture behavior of SINs has been examined at a displacement rate of 10 mm/sec using a three-point bend specimens. As shown in Figure 7, three basic types of fracture behavior are identified according to the increase in PU content. The shape of the load–displacement curves are associated with different types of crack growth behavior.[38,39] Unmodified crosslinked PMMA shows a loading curve with no detectable decrease in gradient before the maximum load, at which point the crack propagates unstably, causing a rapid

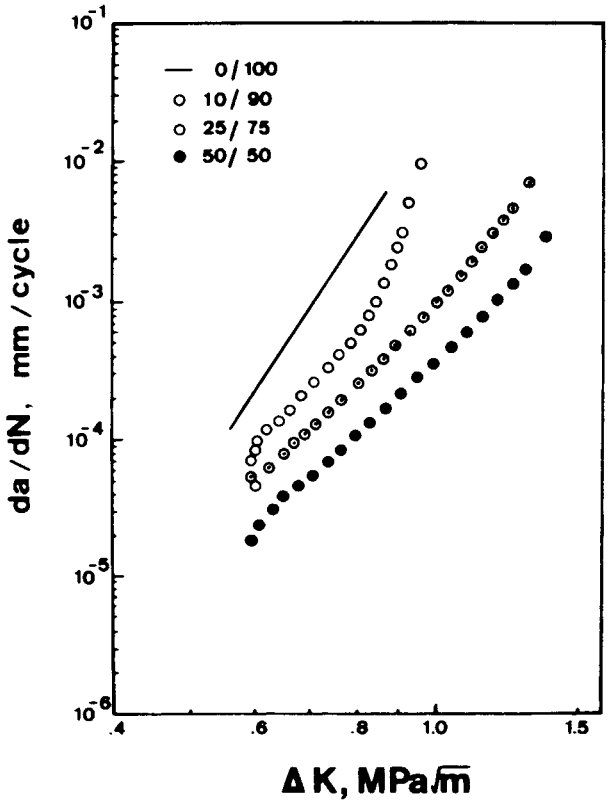

Fig. 5. Fatigue crack growth rates for PU/PMMA SINs.

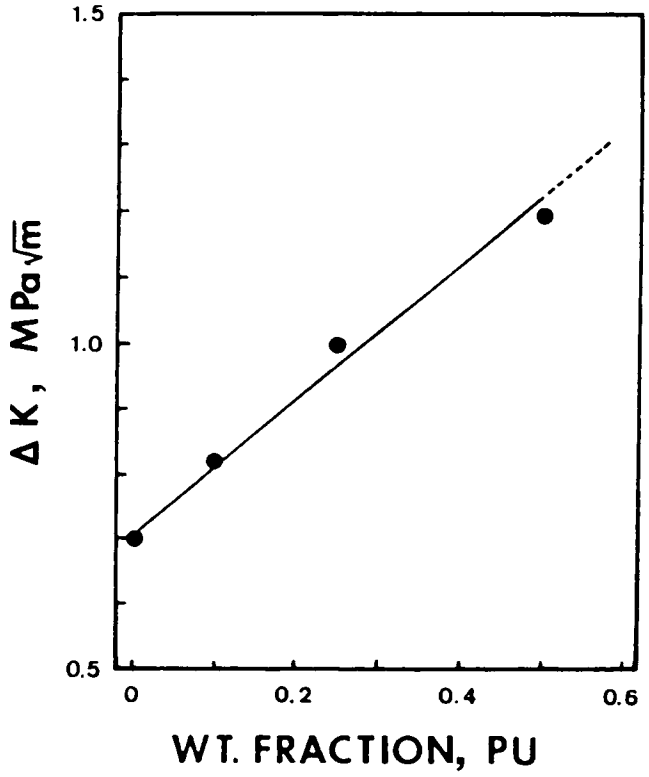

Fig. 6. Effects of composition of PU/PMMA SINs on ΔK^* (at $da/dN = 10^{-3}$ mm/cycle).

load drop (brittle crack growth). In the case of 10/90 and 25/75 SINs, the load rises almost linearly until the maximum value and drops relatively slowly as the crack propagates along the specimen (transition from brittle to ductile crack growth). On the other hand, the 50/50 SIN shows a different load–displacement behavior. While the load increases linearly at first, it becomes

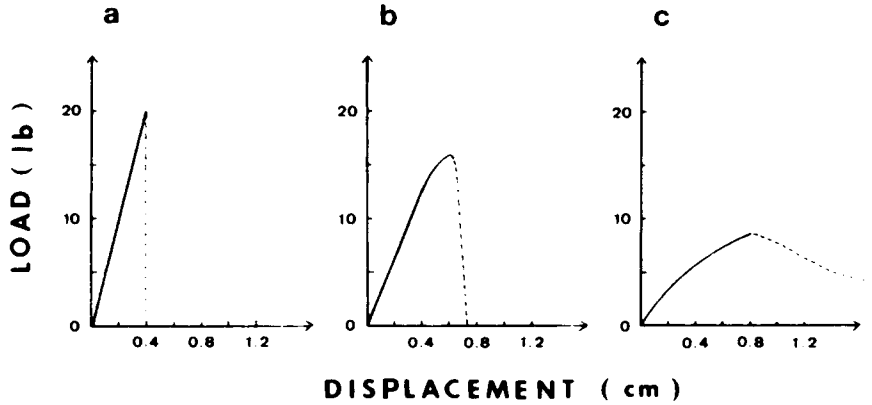

Fig. 7. Load displacement curve for PU/PMMA SINs: (a) crosslinked PMMA; (b) PU/PMMA 25/75 SIN; (c) PU/PMMA 50/50 SIN.

nonlinear before the maximum load as the crack extends stably for a considerable distance (ductile crack growth).

Table I shows that values of fracture toughness K_{1c} increase with increasing PU content; this is consistent with the trend observed in the maximum value of ΔK attained prior to fracture (Fig. 5).

Fractography

Fracture surface studies showed the phenomenon of stress whitening, caused by light scattering due to inhomogeneities or voids generated in the polymer during the fracture process. The size of the stress-whitened region increases with the content of PU. In glassy thermoplastics, such inhomogeneities or microvoids often arise from the initiation and growth of crazes, from shearing, or from rubber cavitation. Donald and Kramer[40] have shown that there is a transition from a crazing to a shear yielding mechanism as the length of the chains between physical entanglements or crosslinks decreases. Thus, in thermosetting resins, there is no evidence of crazing.[39] When the crosslink density is very high or the length of chain between chain entanglements (in the present case, crosslinks and interpenetration) is comparatively short, crazing will be suppressed. Therefore, microvoid formation is expected to involve shearing or cavitation rather than crazing.

Cavitation, which is thought to be around the PU domain [note small holes in Fig. 8(a)] and localized shear deformation are seen in Figure 8. In the case of SINs, the interpenetration of two networks, together with their own crosslinks, aids in the suppression of the crazing. Thus, microvoids are produced by cavitation presumed around the rubbery particles during FCP,

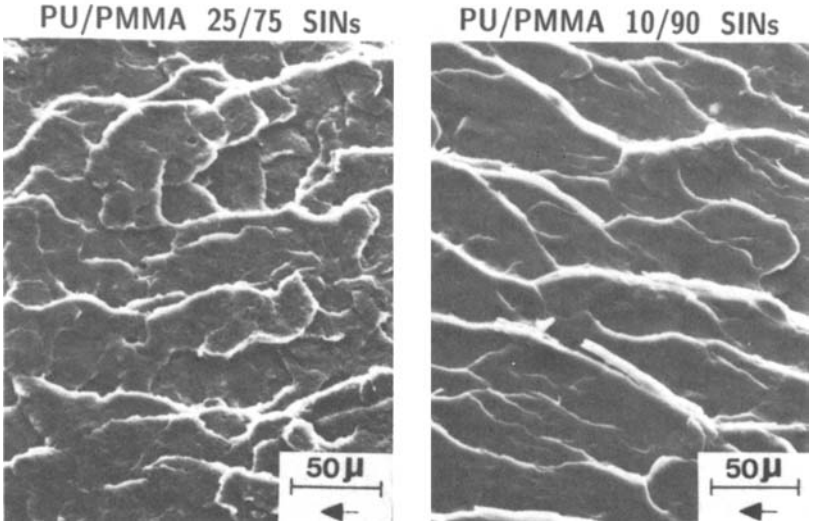

Fig. 8. Scanning electron micrograph of fracture surfaces for PU/PMMA SINs: (a) 25/75 SIN, $\Delta K = 0.70$ MPa$\sqrt{\text{m}}$; (b) 10/90 SIN, $\Delta K = 0.72$ MPa$\sqrt{\text{m}}$.

together with localized plastic deformation due to interaction between the stress field ahead of the crack and the rubber particles. Goodier[41] suggested that the maximum stress concentration occurs at the equator of a rubbery particle. Assuming the particle is well-bonded to the matrix, this stress is triaxial tension. Rubbers are commonly found to undergo cavitation quite readily under the action of a triaxial tensile stress field. However, Figure 8 shows that the extent of the cavitation is relatively small. The dominant factor for the energy dissipating deformation that occurs in the vicinity of the crack tip of a propagating crack is presumably localized plastic deformation.

When this localized plastic deformation is examined in detail, there are several interesting features. Robertson and Mindroiu[42] explained complex fracture surfaces of thermosets based on the hypothesis of an instability of the propagating crack front that produces a "crack fingering" ahead of the nominal crack front. These fingers may lose coherence and move off in different directions when the stress field is inhomogeneous. Thus, an abrupt change in modulus when the crack encounters dispersed PU domains in PU/PMMA SINs is believed to divide a crack into a pair of cracks with each on a different plane.[43,44] Once a crack bifurcates, there is little tendency for cracks to rejoin, and, therefore, the pair of cracks continue on different planes for considerable distances without breaking the intervening membrane to reconnect. The resulting large separations between the crack planes of adjacent fingers yield large steps and welts when the intervening material is finally broken through. The fracture surface of 10/90 SIN in Figure 8(b) shows these steps and welts as the heavy shadows and the complete whiteness, respectively. However, 25/75 SIN shows somewhat different fracture surfaces. The fracture surface shows only irregular patch pattern in Figure 8(a). Finally, in the case of 50/50 SIN (not shown) the fracture surfaces show evidence of pronounced ductility, having an almost torn appearance.

DISCUSSION

Part I in this series discussed SINs prepared by a one-shot procedure in which the PU reactants were mixed with MMA plus a crosslinking agent and cured simultaneously.[26] A single and broad transition, indicative of a microheterogeneous morphology, was observed. In comparison, SINs prepared by the prepolymer procedure described herein exhibit a slightly broader glass transition region, suggesting a greater extent of phase separation. Also, the one-shot materials were more transparent than the corresponding prepolymer materials, indicating smaller domain sizes and/or greater molecular mixing.

In sequential IPNs and SINs alike, phase domain size is controlled by which of two phenomena happen first during the polymerization: gelation or phase separation. If gelation happens first, the network tends to hold the two components together; the resulting domains tends to be smaller, and/or ill-defined. If gelation happens after phase separation, the crosslinks tend to hold the domains apart, and the phases are larger, and/or better defined. While the details of the order are not known for the present case, it may be that the longer initial chains in the chain-extended prepolymer case cause phase separation to happen slightly earlier in the polymerization, perhaps

before or just at the gelation stage. As previously noted, it was observed that the viscosity was significantly increased when one equivalent weight of PPG was prepolymerized with two equivalent weights of MDI. This indicates that there was significant chain extension which resulted in the much longer initial chains. With the two identical overall recipes, the principal difference lies in the distribution of the crosslinks. In the one-shot synthesis, the crosslinks are nearly random, whereas in the prepolymer case, the crosslinks tend to be clumped together between chain extended prepolymer segments. In any case, the prepolymer synthesis results in somewhat better defined domains, which in turn may yield greater toughness to the material. Indeed, both energy absorption and FCP resistance were greater for the SINs prepared by prepolymer procedure.

Translucency of the SIN samples also suggests that there is some degree of phase separation, since an homogeneous solution is usually transparent (but, of course, may be colored) whereas a nonhomogeneous mixture is turbid unless the components of the mixture have identical refractive indexes.[45]

The original interpenetration of a single and broad transition in the dynamical data (Fig. 1 and 2) was that different regions of space had different compositions, each yielding its own glass transition temperature.[2] Such a morphology is sometimes called "microheterogeneous." If the minimum volume required for independent contributions to the relaxation spectrum is the same or smaller than that required to yield homogeneous overall compositions, a broad transition will result.

Alternately, Lipatov et al.[46] suggested that an intermediate T_g arises from extensive interphase material. Since local concentration fluctuations would be expected to be rife in the phase boundary region, the whole material may be considered a macroscopic interphase structure. In any case, this single and broad transition is believed to be typical of a "semimiscible" system which has microheterogeneity in that an infinite number of domains of differing compositions exist. The term "semimiscibility" covers the range between partial mutual solubility and total molecular solution. Thus, it is a relative measure of the degree of heterogeneity of the polyblends. Thermodynamically, such systems must have an almost zero free energy of mixing, or perhaps the free energy of mixing varies slightly with minor compositional changes.

Figure 3 shows that T_g values of the SINs are apparently lower than theory. However, this may be an artifact arising from the phase separation and concomitant broad temperature range of the loss modulus. Midrange compositions exhibited shoulders (not shown). It must be noted that storage modulus of the prepolymer IPNs were lower than the corresponding one-shot IPNs.[28]

The increase in the FCP resistance with increasing PU content was observed in Figure 5. Hertzberg and Manson[26] noted that the fatigue response of rubber-toughened plastics is dominated by the characteristically higher level of viscoelastic damping relative to that of the unmodified plastics. Thus, the increased FCP resistance of the SINs is believed to arise from the ability of the PU network to dissipate energy. Indeed, Table I shows that E(abs) was significantly increased with PU content. Skibo et al.[37] examined the effect of rubber content on FCP behavior. While a decrease in modulus due to an increase in rubber content tends to increase crack growth rates, a decrease in

yield strength, σ_y, is beneficial as a result of the associated increase in the damage zone dimension (γ_y) given by the Dugdale equation[47]:

$$\gamma_y = \frac{\pi K^2}{8\sigma_y^2} \tag{7}$$

Also, localized heating in the damage zone would act to blunt the crack tip, thereby yielding a lower growth rate. However, at higher concentration of rubber ([PU] > 50%), the significant decrease in modulus as the PU content increases evidently overcame the beneficial effects of energy dissipation. Instrumentation specifically designed for elastomers will have to be used to evaluate the highly elastomeric systems. In any case the net effect of rubber on growth rates will be determined by a dynamic energy balance between the ability of the rubber to generate energy-dissipating processes at the crack tip, and softening of the bulk polymer.

Interestingly, the fracture surface shows different behavior between the SINs depending on the PU content such as steps and welts (10/90 SIN), irregular patch (25/75), and torn appearance (50/50). This can be explained by considering the local stress fields around the PU domains under the applied stress. Larger amount of PU encorporation causes stress fields which are much more complex so that the crack planes of adjacent fingers rejoin before they continue to grow on different planes. Thus, irregular patches are shown in 25/75 SIN instead of steps and welts. Also, when the PU content increases, the glass temperature region approaches the test temperature. Then, cracks undergo relatively ductile growth, thereby showing an almost torn appearance. Indeed, in the case of 50/50 SIN, the measurement temperature is near the glass transition region. This is consistent with fracture behavior in which the load-displacement shows brittle, brittle-ductile transition, ductile crack growth depending on the PU content (Fig. 7).

CONCLUSIONS

The SINs prepared by a prepolymer procedure in which a PU network was combined with a PMMA network appear to have a single and broad class transition. The 25°C shear modulus behavior of the SINs are approximately described by the Davies model and the Budiansky model, which indicates that dual-phase continuity prevails in the midrange compositions.

While energy absorption measured from dynamic properties and pendulum impact tests increases directly with PU content, FCP resistance and fracture toughness increase with PU content up to 50%, since crack growth rates are determined by a dynamic energy balance between the ability of the rubber to generate energy-dissipating processes at the crack tip and softening of the bulk polymer. Three basic types of fracture behavior (brittle–transition–ductile crack growth) were observed, depending on the PU content. The micromechanism of failure involves the generation of extensive stress whitening associated with the cavitation and localized shear deformation rather than crazing.

The authors wish to acknowledge support from the National Science Foundation Materials Division, Grant No. DMR-8412357, Polymers Program.

References

1. D. Klempner and L. Berkowski, "Interpenetrating Polymer Networks," in *Encyclopedia Polymer Science and Engineering Vol. 8*, 2nd ed., Wiley-Interscience, New York, 1987.

2. L. H. Sperling, *Interpenetrating Polymer Networks and Related Materials*, Plenum, New York, 1981.

3. L. H. Sperling, in *Multicomponent Polymer Materials*, D. R. Paul and L. H. Sperling, Eds., ACS Adv. Chem. Ser. No. 211, Am. Chem. Soc., Washington, D.C., 1986.

4. A. Morin, H. Djomo, and G. C. Meyer, *Polym. Eng. Sci.*, **23**, 394 (1983).

5. D. Klempner, *Angew. Chem. Int. Ed. Engl.*, **17**, 97 (1978).

6. H. L. Frisch, K. C. Frisch, and D. Klempner, *Pure Appl. Chem.*, **53**, 1557 (1981).

7. D. J. Hourston, M. G. Huson, and J. A. McCluskey, *J. Appl. Polym. Sci.*, **31**, 709 (1986).

8. D. Klempner, L. Berkowski, and K. C. Frisch, *Rubber World* **187**(9), 16 (1985).

9. M. C. O. Chang, D. A. Thomas, and L. H. Sperling, *J. Polym. Sci. Polym. Phys. Ed.*, **26**, 1627 (1988).

10. D. J. Hourston and J. A. McCluskey, *J. Appl. Polym. Sci.*, **31**, 645 (1986).

11. D. Klempner, C. L. Wang, M. Ashtiani, and K. C. Frisch, *J. Appl. Polym. Sci.*, **32**, 4197 (1986).

12. R. B. Fox, J. L. Bitner, J. A. Hinkley, and W. Carter, *Polym. Eng. Sci.*, **25**(3), 157 (1985).

13. M. Akay, S. N. Rollins, and E. Riordan, *Polymer*, **29**, 37 (1988).

14. J. S. Lin and J. A. Manson, *Proc. 45th Annu. Tech. Conf. SPE*, 478 (1987).

15. N. Devia, L. H. Sperling, J. A. Manson, and A. Conde, *Polym. Eng. Sci.*, **19**, 878 (1979).

16. G. C. Meyer and P. Y. Mehrenberger, *Eur. Polym. J.*, **13**, 383 (1977).

17. D. J. Hourston and Y. Zia, *J. Appl. Polym. Sci.*, **29** 2951 (1984).

18. (a) S. C. Kim, D. Klempner, K. C. Frisch, W. Radigan, and H. L. Frisch, *Macromolecules*, **9**, 263 (1976); (b) *ibid.*, 1187 (1976).

19. D. J. Hourston and Y. Zia, *J. Appl. Polym. Sci.*, **28**, 3745 (1983).

20. G. Allen, M. J. Bowden, D. J. Blundell, F. G. Hutchinson, G. M. Jeffs, and J. Vyvoda, *Polymer*, **14**, 597 (1973).

21. G. Allen, M. J. Bowden, G. Lewis, D. J. Blundell, and G. M. Jeffs, *Polymer*, **15**, 13 (1974).

22. D. J. Blundell, G. W. Longman, G. D. Wignall, and M. J. Bowden, *Polymer*, **15**, 33 (1974).

23. (a) H. Djomo, A. Morin, M. Damyanidu, and G. C. Meyer, *Polymer*, **24**, 65 (1983); (b) S. R. Jin, J. M. Widmaier, and G. C. Meyer, *Polymer*, **29**, 346 (1988).

24. Y. Lipatov, L. Karabanova, L. Sergeeva, L. Gorbach, and S. Skiba, *Vysokomol. Soedin. B. Krat. Soobshch.*, **29**(4), 274 (1986).

25. C. Mai and G. P. Johari, *J. Polym. Sci. Polym. Phys. Ed.*, **25**, 1903 (1987).

26. R. W. Hertzberg and J. A. Manson, *Fatigue in Engineering Plastics*, Academic, New York, 1980.

27. S. Qureshi, J. A. Manson, L. H. Sperling, and C. J. Murphy, in *Polymer Applications of Renewable Resource Materials*, C. E. Carraher, and L. H. Sperling, Eds., Plenum, New York, 1983.

28. T. Hur, J. A. Manson, and R. W. Hertzberg, in *Crosslinked Polymers*, R. A. Dickie. S. S. Labana, and R. S. Bauer, Eds., ACS Symp. Ser. No. 367, Am. Chem. Soc., Washington, D.C., 1988.

29. J. D. Ferry, *Viscoelastic Properties of Polymers*, 3rd ed., Wiley, New York, 1980.

30. P. C. Paris and F. Erdogan, *J. Bas. Eng. Trans. ASME. Ser.*, **D85**(4), 528 (1963).

31. A. J. Kinloch and R. J. Young, *Fracture Behavior of Polymers*, Applied Science, London and New York, 1983.

32. T. G. Fox, *Bull. Am. Phys. Soc.*, **1**, 1 (1956).

33. J. M. Pochan, C. L. Beatty, and D. F. Hinman, *Macromolecules*, **11**, 1156 (1977).

34. M. Takayanagi, *Mem. Fac. Eng. Kyushu Univ.*, **23**, 11 (1963).

35. W. E. Davies, *J. Phys. D*, **4**, 318 (1971).

36. B. Budiansky, *J. Mech. Phys. Solids*, **13**, 223 (1965).

37. M. D. Skibo, J. A. Manson, S. M. Webler, R. W. Hertzberg, and E. A. Collins, *Am. Chem. Soc. Symp. Ser.*, **95**, 311 (1979).

38. B. W. Cherry and K. W. Thomson, *J. Mater. Sci.*, **16**, 1913 (1981).
39. A. J. Kinloch, S. J. Shaw, D. A. Tod, and D. L. Hunston, *Polymer*, **24**, 1341 (1983).
40. A. M. Donald and E. J. Kramer, *J. Mater. Sci.*, **17**, 1871 (1982).
41. J. N. Goodier, *Trans. Am. Soc. Mech. Eng.*, **55**, 39 (1933).
42. R. E. Robertson and V. E. Mindroiu, *Polym. Eng. Sci*, **27**(1), 55 (1987).
43. A. J. Kinloch, D. L. Maxwell, and R. J. Young, *J. Mater. Sci. Lett.*, **4**, 1276 (1985).
44. A. J. Kinloch, D. L. Maxwell, and R. J. Young, *J. Mater. Sci.*, **20**, 4169 (1985).
45. O. Olabisi, L. M. Robeson, and M. T. Shaw, *Polymer–Polymer Miscibility*, Academic, New York, 1979.
46. Yu. S. Lipatov, T. S. Chramova, L. M. Sergeva, and L. V. Karabanov, *J. Polym. Sci. Polym. Chem. Ed.*, **15**, 427 (1977).
47. D. S. Dugdale, *J. Mech. Phys. Solids*, **8**, 100 (1960).

Received February 3, 1989
Accepted March 20, 1989